Pure Sciences International Journal of kerbala

Year:2024 Volume : 1 Issue : 2 ISSN: 6188-2789 Print 3005 -2394 Online

Mohammed Hasan Hameed, Numerical Solution of The Two-dimensional Diffusion Logistic Model(Crank-Nicolson), Pure Sciences International Journal of Kerbala, Vol. 1 No. 2 (*2024*) 17-24

2024 ,Volume 1 , Issues 2 PSIJK 17-24

Pure Sciences International Journal of Kerbala

Journal Homepage:https://journals.uokerbala.edu.iq/index.php/psijk

Numerical Solution of The Two-dimensional Diffusion Logistic Model (Crank-Nicolson)

Mohammed Hasan Hameed[1]

[1] Ministry of Education / Babylon Education Directorate

P A P E R I N F O

Paper history:
Received 28 March 2024
Accepted 22 May 2024
Published 30 June 2024

Keywords:
fourth-order reaction-diffusion 1, diffusion logistic model (Crank-Nicolson) 2

A B S T R A C T

The paper presents a detailed numerical analysis of the nonlinear fourth-order fractional reaction-diffusion equation using the compact difference method. The introduction of the fourth-order fractional derivative adds additional complexity to the equation, making its analytical solution challenging. Therefore, a numerical approach becomes necessary to understand the behavior of the equation and obtain approximate solutions. The compact difference method, known for its accuracy and efficiency in solving differential equations, is used to discretize the spatial and temporal derivatives of the equation. The fractional derivatives are approximated using suitable fractional difference operators. The resulting system is solved iteratively using appropriate numerical techniques. The study delves into a reaction-diffusion model utilized in brain gliomas, incorporating two different diffusion functions. In order to achieve a thorough comprehension, the analysis is broadened to encompass various types of tissue environments. Diverse scenarios are scrutinized, with the diffusion coefficient staying consistent to depict a uniform tissue environment. Furthermore, instances where the diffusion coefficient changes spatially are explored, bringing heterogeneity into the model. This spatial diversity accommodates the differing characteristics of distinct regions within the brain. Following this, the examination is expanded to include heterogeneous tissue environments in two dimensions.

NOMENCLATURE			
BR	*v*	(Đ, μ, a, b, H)	a parameter in the two-dimensional simulation
Nt	time step size in the accuracy test		
Nx	spatial grid size in the accuracy test		
T	final time in the evaluation		
		Greek Symbols	
Subscripts		Φ	Phi
n	used in the context of time steps, e.g., $\cup^n$	ε	Epsilon
x, y	representing spatial dimensions, e.g., C(x, y, 0)	μ	Mu
t	representing time, e.g., t = 50, t = 100, t = 650, t = 850	√	Square root symbol
Nx, Nt	representing spatial and time grid sizes, e.g., Nx × Nt		
L2, L1	representing norms, e.g., L2Error, L1Error		

1. INTRODUCTION

A fourth-order compact difference method is a numerical time-fractional 4th-order reaction-diffusion equation. This method approximates the solution of the equation by discretizing the domain and using finite difference approximations to represent the derivatives. The block_centered finite_difference method is a specific type of 4th-order compact difference method that has been applied to various types of differential equations, including parabolic equations . technique used to solve differential equations, specifically the non linear. This method is known for its ability to

*Corresponding Author Institutional Email: *mhmdhsnhmydhmwdalsltany@gmail.com* (Mohammed Hasan Hameed)

approximate the exact solution and its derivatives while preserving the local conservation of the problem. It is particularly useful for problems with Neumann boundary conditions, as it eliminates the need to separately consider the numerical solution near the boundary. The time-fractional 4rth-order reactiɒn-diffusiɒn equation is a mathematical model that describes the behavior of certain physical and biological systems. It combines the concepts of reaction and diffusion, as well as fractional derivatives that capture the history dependence of the system. The time-fractional derivative is especially effective in accurately describing dynamic processes with time variables. The block_centered finite-difference method for the time-fractional 4th-order reactiɒn-diffusiɒn equatiɒn has not been widely studied in the literature. However, there have been developments in related areas, such as the block_centered finite_difference method for parabolic equations with fractional-order time derivatives. These studies have demonstrated the stability and convergence of the method and provided error estimations for the approximate solution and its derivatives. In summary, the 4th-order compact difference method, specifically the block-centered finite-difference method, is a promising numerical technique for solving the nonlinear time-fractional 4th-order reaction-diffusion equation. Further research is needed to fully explore its potential and develop efficient algorithms.

2. EVALUATION OF CONVERGENCE FOR THE F_TRACKING METHOD IN A ONE-DIMENSIONAL MODEL

In the "logistic diffusion model" (2.1)-(2.5) with parameter values (Đ, μ, a, b, H) = (0.40, 10.1, 1.1, 1.1, 1.1) and initial condition ∪0 = cos(x^2), we investigate the effect of varying the temporal size while maintaining a fine spatial resolution. The convergence and error analysis of the " diffusion logistic model(crank-nicolson) " are presented in Table 2.1 for a the concluding time of t_end = 1. The discrepancy is calculated, as the disparity between the numerical solutiɒn and the exact solutiɒn, whenever available. In cases where the exact solutiɒn is not provided, the solutiɒn obtained employing a meticulous level of detail is considered as the a benchmark or precise solutiɒn. Notably, 2^{sd}- In all instances, a convergence of higher order is observed in the spatial dimension.

TABLE 1. Accuracy test of U of diffusion logistic

Nx × Nt	L2Error	Order (*t*)	L1Error	Order
61×2e06	4.10e-003	4.4e-03		
121×2e06	9.40e-004	2.250	9.35e-004	2.14
241×2e06	2.20e-004	2.160	2.10e-004	2.10
481×2e06	4.36e-05	2.360	4.08e-05	2.33
961×2e06	Reference			

TABLE 2. Accuracy results for diffusion logistic model of one dimension

Nx × Nt	L2Error	Order (*t*)	L1Error	Order
61×2e06	1.68e-01	4.28e-02		
121×2e06	2.72e-02	2.63	9.40e-03	2.19
241×2e06	6.20e-04	2.62	4.09e-04	2.36
481×2e06	4.36e-05	2.84	4.08e-05	2.33
961×2e06	Reference			

Analysis of convergence the F- methodology for stabilizing the one-dimensional: Considering the population spread with logistic diffusion medal (2.1)-(2.5) with parameter values (Đ, μ, x, y, H0) = (0.400, 10.1, 1.1, 1.1, 1.1) and initial condition U0 = cos(x^2), we investigate the impact of varying the temporal size while maintaining a fine spatial resolution. Table 2.2 presents an examination of the error (both L-2 and L11 norms) and the cɒnvergence behavior of the "front-fixing method", with a the concluding time of t_end = 1. As anticipated, a 2^{sd}- convergence of a certain degree in the spatial dimension is readily noticeable .

3. CONVERGENCE TEST FOR DIFFUSION LOGISTIC MODEL(CRANK-NICOLSON) OF 2D MODEL WITH RADIAL-SYMMETRY

We investigate the 2D The logistic diffusion model exhibiting radial symmetry, characterized by parameters (Đ, μ, x, y, H) = (0.400, 10.1, 1.1, 1.1, 0.54), and an initial condition of ∪0 = cos(r/2). This model serves as a test case for evaluating the performance of the F-tracking- method. In Table 3.1, we examine the discrepancy (both in terms of L_2 and L_1 norms) and the spatial convergence order of the F-tracking - method's solution, with a final time of T = 0.0100. Once again, we observe a 2nd- convergence rate in the spatial dimension. The convergence test for the F-fixing method applied to the 2D model with radial symmetry is presented in Table 3.2, showing the accuracy results obtained.

TABLE 3. Accuracy test of U of diffusion logistic model(Crank-Nicolson)

Nx × Nt	L2Error	Order	L_∞Error	Order
71×2e04	6.50e-04		2.71 e-04	
141×2e04	1.40e-04	2.20	5.35e-04	2.14
281×2e04	3.20e-05	2.15	1.10e-04	2.10
561×2e04	6.36e-06	2.38	2.08e-05	2.35
1121×2e04	Reference			

TABLE 4. Accuracy results for diffusion logistic model (Crank-Nicolson) of one-dimensional

Nx × Nt	L2Error	Order (*t*)	L1Error	Order
71×2e05	3.68e-01			
141×2e05	6.72e-02	2.15	1.40e-03	2.22
241×2e05	1.20e-04	2.14	2.09e-04	2.14
581×2e05	3.36e-05	2.34	2.08e-05	2.35
1121×2e05	Reference			

In this section, we conduct drawing a parallel between, the diffusion logistic model(Crank-Nicolson) and the diffusion logistic model for simulating the 2^D population spread through logistic diffusion exhibiting radial symmetry. The model is characterized by parameters (Đ, μ, x, y, H0) = (0.400, 10.1, 1.1, 1.1, 1.1), an initial condition of $\cup 0 = \cos\left(\frac{r}{2}\right)$, and a dimensional magnitude of h = 0.00625. It Illustrates that the" diffusion logistic model(Crank-Nicolson) " closely aligns with the one-dimensional when applied to the 2^D spread of diffusion logistic model(crank-nicolson) with radial symmetry. To analyze the approach based on level sets for the 2D model, we perform numerical tests and convergence analysis. The approach based on level sets is employed to study the two-dimensional logistic diffusion model displaying radial symmetry, described by equations (2.39)-(2.43) with parameters (Đ, μ, x, y) = (0.400, 10.1, 1.1, 1.1). The initial level set function represents a circle with a radius of 1, and the initial condition is depicted using a red dotted curve to visualize the simulated species boundary. Additionally, a blue circle is introduced to indicate the resemblance of the evolving boundary with a circle. The measurement of the circumference of the blue circle, denoted as R, is calculated as the mean separation among the intersection points of ϕ(t) with the x-axis and y-axis at the boundary and the point of origin, i.e., R = √(x^2 + y^2), where (x, y) ∈ ϕ(t) represents all the intersection points of ϕ(t) with the x-axis and y-axis. According to reference [13], the resolution of the equations. (2.21)-(2.24) is unique and exhibits radial symmetry. It displays the progression of ∪(t, x, y) and ϕ(t), demonstrating a perfect match between the blue circle and the red dotted curve, indicating the preservation of the geometric shape of the boundary ϕ(t). Furthermore, it is noticeable that .∪(t, x, y) exhibits radial symmetry, similar to ∪0. Our attention is directed towards the measurement of the boundary's radius. ϕ(t), denoted as H(t), and utilize ∪(t, r) = ∪(t, x, y) to examine the spatial accuracy order of the approach based on level sets technique. The assessment of the convergence of the solution for u(r) at T = 0.100 and the front H(t) can be performed.

4. COMPARISON AND CONVERGENCE ANALYSIS.

Observing the comparison between the level set method and the F- tracking -method, we consider different spatial sizes, namely h = 0.02500, h = 0.012500, h = 0.0062500, and h = 0.00312500. The obtained results are then compared to those of the F- a tracing approach using identical initial conditions configuration and step size h = 0.00312500. The comparison clearly demonstrates a high degree of consistency between the level set method and the front tracking method, indicating their agreement with each other. To further assess the performance of the level set method, Table 1 provides an analysis of the error (both L-2 and L-1 norms) and the convergence order for the solution gained through employing the level set technique, culminating at a designated endpoint of T = 0.1. The table presents findings indicating the convergence rates in regard pertaining to both the solution u and the leading edge H(t) fall within the range of 1 to 2.

TABLE 5. Accuracy test of U of diffusion logistic model(crank-nicolson)

Nx × Nt	L2Error	Order	L_∞Error	Order
28×28×161	5.50e-04		9.71 e-04	
58×58×166	3.40e-04	0.20	5.35e-04	0.14
112×112×2530	1.20e-05	1.15	2.10e-04	1.10
240×240×1050	4.36e-06	1.38	7.08e-05	1.35
551×551×41951	Reference			

TABLE 6. Accuracy results for diffusion logistic model(crank-nicolson) of one- dim

Nx × Nt	L2Error	Order (*t*)	L1Error	Order
28×28×161	4.68e-01			
58×58×166	2.72e-02	1.15	5.40e-03	1.22
112×112×2530	8.20e-04	1.14	2.09e-04	1.14
240×240×1050	2.36e-05	1.34	3.08e-05	1.35
551×551×41951	Reference			

5. NUMERICAL DICHOTOMY THE DICHOTOMY BETWEEN EXPANSION AND DISAPPEARANCE

Example 1 : The one-dimensional diffusive logistic model with a free boundary, as formulated in reference [14], is used to describe the population density of the invasive species U(t, x), where it depends on time t and the spatial variable x, as stated in the following expression:

$$\frac{\partial \cup}{\partial t} - \frac{D\,\partial^2 \cup}{\partial x^2} = \cup(a - b\cup), t > 0, \quad x \in (0, H(t)], \qquad (2.1)$$

In addition to the boundary conditions, the text emphasizes the importance of considering all relevant factors

$$\frac{\partial \cup}{\partial x(t,0)} = 0, \cup (t, H(t)) = 0, t > 0, (2.2)$$

the Stefan condition

$$H^0(t) = -\frac{\mu \partial \cup}{\partial x(t, H(t))}, t > 0, (2.3)$$

and the initial conditions

$$H(0) = H^0, \cup (0, x) = \cup^0 (x), 0 \leq x \leq H^0. (2.4)$$

The function $\cup_0(x)$ fulfills the subsequent properties:

$$\cup^0 (x) \in C^2([0, H^0]), \cup^{0\prime} (0) = \cup^0 (H^0) = 0, \cup^0 (x) > 0, 0 \leq x < H^0. (2.5)$$

H(t) represents the mysterious shifting boundaries within which the population is dispersed within the range [0, H(t)]. D > 0 is the rate of dispersal, with the parameters a and b indicating the intrinsic diffusion rate and intraspecific competition within the population, respectively. The parameter $\mu > 0$. The Stefan condition (2.3) specifies the constant of proportionality that relates the population gradient at the front to the velocity of the advancing boundaries.

Example 2 :of the free boundary logistic diffusion model (2.1)-(2.5), with parameter values (D, μ, a, b, H_0) = (1, 5, 1, 1, 0.496) and $U^0 = \cos\left(\frac{\pi x}{2H^0}\right)$, it can be observed from Figure 2.12 the spreading behavior that occurs even when H_0 = 0.496, which is less than the value of L = 1.571.

As another example, in the free boundary logistic diffusion model (2.1)-(2.5), we set the parameter values as follows: D = 1, μ = 5, a = 1, b = 1, and H_0 = 0.496. The initial function is given by $\cup^0 (x) = \left(\frac{1}{2}\right)\cos\left(\frac{\pi x}{2H^0}\right)$. In this example, we keep the parameter values the same as in the previous example except that we decrease the initial value ∪.

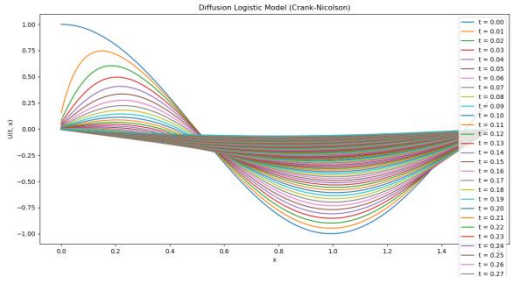

6. REACTION-DIFFUSION EQUATION IN TWO DIMENSIONS

In this section, an evaluation of the stability of the linear system will be performed using the von Neumann technique of finite difference method derived from the two-dimensional equation of the linear model. The evaluation includes a spread component that increases rapidly and acts as an interactive term.

$$\frac{\partial t}{\partial C} = \frac{\frac{\partial x}{\partial} D(x) \partial x}{\partial C} + \frac{\frac{\partial y}{\partial D(x) \partial y}}{\partial C} + \rho C. \quad (32)$$

From the construction of the derivative of the two-dimensional interaction and interaction equation, which includes the coupled covariant isolation function, different terms can be reformulated to indicate a component of the term. Negotiate the system of equation (32) in a completely different way:

$$\begin{aligned} 1 + \frac{2D(x_i)\Delta t}{h^2} + \frac{2D(x_i)\Delta t}{k^2} - \frac{\rho \Delta t^2}{2} C_{\{n+1,i,j\}} \\ - \frac{D(x_i)\Delta t}{h^2\left(C_{\{n+1,i-1,j\}} + C_{\{n+1,i+1,j\}}\right)} \\ - \frac{D(x_i)\Delta t}{k^2\left(C_{\{n+1,i,j-1\}} + C_{\{n+1,i,j+1\}}\right)} \\ = 1 - \frac{2D(x_i)\Delta t}{h^2} - \frac{2D(x_i)\Delta t}{k^2} \\ + \frac{\rho \Delta t^2}{2} C_{\{n,i,j\}} \\ + \frac{D(x_i)\Delta t}{h^2\left(C_{\{n,i+1,j\}} + C_{\{n,i-1,j\}}\right)} \\ + \frac{D(x_i)\Delta t}{k^2\left(C_{\{n,i,j+1\}} + C_{\{n,i,j-1\}}\right)} \\ - \frac{D(x_i)\Delta t}{4h}\left((Cx)_n^{\{i+1,j\}} - (Cx)_n^{\{i-1,j\}}\right) \\ - \frac{D(x_i)\Delta t}{4h}\left((Cx)_{\{n+1\}}^{\{i+1,j\}} - (Cx)_{\{n+1\}}^{\{i-1,j\}}\right) \\ - \frac{D(x_i)\Delta t}{4k}\left((Cy)_n^{\{i,j+1\}} - (Cy)_n^{\{i,j-1\}}\right) \\ - \frac{D(x_i)\Delta t}{4k}\left((Cy)_{\{n+1\}}^{\{i,j+1\}} - (Cy)_{\{n+1\}}^{\{i,j-1\}}\right) \\ + \frac{K(x_i)\Delta t^2}{2}\left((Cx)_n^{\{i,j\}} + (Cx)_{\{n+1\}}^{\{i,j\}}\right). \end{aligned}$$

The compact solutions algebraic systems linked to the finite difference approximation (23) that can be rewritten in a different manner offer several advantages. One of the most compelling reasons is the presence of the innate characteristic of generating the resulting system of equations which contains symmetric coefficient matrices equations. Moreover, these matrices possessing a comparatively smaller range of frequencies compared to decreased bandwidth that stems from non-compact solutions are particularly advantageous since they result in more efficient and computationally feasible solutions. Now, let us delve into the methods for solving these algebraic systems using the following notations:

$$\cup = [C1, C2, \dots, Cm],$$
$$\cup x = [(Cx)1, (Cx)2, \dots, (Cx)m]$$

The matrix representation of the system of equations is as follows:

$$A1U \cup^{n+1} = B1(\cup^n, \cup x^n, \cup x^{n+1}) \quad (34)$$

Once the approximation of ∪^n has been achieved at any given time step, ∪ x^n can be obtained by solving tridiagonal systems

$$A2 \cup x^n = B2 \cup^n \quad (35)$$

Equation (35) represents the matrix form associated with relations (8), which are tridiagonal systems that can be effectively resolved through the use of powerful numerical algorithms. The main goal is to solve the system (23) to estimate the unknown transporter vector ∪^(n+1). Our approach faces significant challenges when incorporating the (n + 1)-the time level gradients of U on the left-hand side of Equation (34). These gradients are only available after determining the transportation parameter at the time level of (n + 1). To overcome this issue, we implement a convergence correction strategy. Despite the large dimensions of the coefficient matrix., we effectively tackled this obstacle by employing the bi-conjugate gradient stabilized (BiCG-Stab) technique, eliminating the necessity for preconditioning.

The convergence condition for the BiCG-Stab iteration is. influenced by the size of the grid and the specific characteristics of the problem at hand. This approach is also applied when simulating other discussed schemes in this research, both in one or two dimensions. In the numerical experiments conducted in one aspect, we made use of an assortment one hundred and one spatial grids spanning from 0 to 50. The time step used was Δt = 0.02 days, which is approximately equivalent to 28.8 minutes. As for the data related to the two-dimensional simulation, the values were as follows .: epsilon = 0.0100, h = 0.500 mm, k = 0.500 mm, and the growth rate ρ = 0.012000 $day^(-1)$. Initially, the particles were placed at the location (x_0, y_0) = (25, 25), and we used a time step Δt of 0.02 days (~28.8 min). The load capacity K was determined to be $62.5\frac{cells}{mm}$, and the maximum value of C(x, y, 0) was $39.89\frac{cells}{mm}$. Throughout the simulation, we maintained fivefold differences in diffusion coefficients between gray matter and white matter: $D_{white} \approx 5D_{gray}$. The proliferation rate ρ was set at $0.01200\ day^{-1}$, according to the model proposed by Swanson and colleagues for high-grade tumors [36]. All calculations were performed at maximum power, with $K = 62.5\frac{cells}{mm}$, and we used the following initial distribution:

$$C(x,0) = \left(\frac{1}{\sqrt{2\pi\epsilon}}\right) * e^{-\left(\frac{1}{2}\right)*\left(\frac{x-x_0}{\epsilon}\right)^2}$$

At the middle of the considered period, the position $x_0 = 25$ mm was determined, and the parameter epsilont was estimated to be 0.0100. When examining the distribution of C(x, 0), a peak appears at $x = x_0$, with a value of about $39.89\frac{cells}{mm}$. This value, called C_0, represents the local density of the tumor of about $39.89\frac{cells}{mm}$ before it begins to spread.

After reviewing Figures 4a and 4b, it becomes clear that the concentration of primary tumor cells significantly decreases from $39.89\frac{cells}{mm^2}$ to $8.2\frac{cells}{mm^2}$ within one day using the known 4O-CEFE method. On the other hand, the concentration remains constant at $10.62\frac{cells}{mm^2}$ using the known IBE method. Figures 5a, 5b, 6a, and 6b demonstrate the concentration of motor neuron tumor cells relative to the variable x using IBE on the left side and 4O-CEFE on the right side. In the simulation, a value of $\rho = 0.0129\, day^{-1}, \Delta t = 0.024$ minutes (approximately 28.8 minutes), and $\Delta x = 0.5\, mm$ were used, covering time periods of $t \in (100, 200)$ and t(1050,1280. In Figure 5b, it is evident that the 4O-CEFE method outperforms the IBE method by t = 200 days, with a tumor cell concentration of $3.95\frac{cells}{mm^2}$ compared to $2.25\frac{cells}{mm^2}$ in the IBE method during the time period of $t \in [1050,1280\ ]$. According to Ozugurlu [23], it took 1470 days using the 4O-CEFE method and 2300 days using the IBE method to reach maximum capacity $\left(K = 62.4989979\frac{cells}{mm^2}\right)$. The data depicted in Figures 6a and 6b showcases the information. It should be noted that the data in Figure 6a only goes up to 1280 days. The value of x_0 was set at 25 mm as the center for the analysis period. The coefficient ϵ is estimated to be approximately 0.0100. The cell distribution C(x, 0) exhibits a peak at $x = x_0$, estimated at around $39.89\frac{cells}{mm^2}$, denoted as C_0, showing the tumor reaching a local density of approximately $39.89\frac{cells}{mm^2}$ before its spread begins.

The research conducted by Ozugurlu [23] aims to compare the results obtained using the IBE method with those obtained using the 4O-CEFE method. By studying Figures 4A and 4B, it becomes evident that the concentration of primary tumor cells significantly decreases from $39.89\frac{cells}{mm^2 to}8.2\frac{cells}{mm^2}$ within one day using the 4O-CEFE method. Meanwhile, the concentration remains constant at $10.62\frac{cells}{mm^2}$ using the IBE method. Figures 5A, 5B, 6A, and 6B illustrate the concentration of motor neuron sarcoma cells with respect to the variable x. The left side represents the IBE method, while the right side represents the 4O-CEFE method. The simulation was performed using the $values\ \rho = 0.012\, day^{-1}, \Delta t = 0.02$ minutes (approximately 28.8 minutes), and Δx = 0.5 mm, spanning the time periods $t \in [100, 200]$ and $t \in [1050, 1280\ ]$. Figure 5B indicates that the 4O-CEFE method outperforms the IBE method by t = 200 days, with a tumor cell concentration of $3.95\frac{cells}{mm^2}$compared to $2.25\frac{cells}{mm^2}$ in the IBE method during the time period $t \in (1050\ , 1280)$. According to Ozugurlu [23], it took 1470 days using the 4O-CEFE method and 2300 days using

the IBE method to reach the maximum capacity $\left(K = 62.4989979 \frac{cells}{mm^2}\right)$, as shown in Figures 6A and 6B. It should be noted that the data in Figure 6A the time frame is restricted to a maximum of 1280 days.

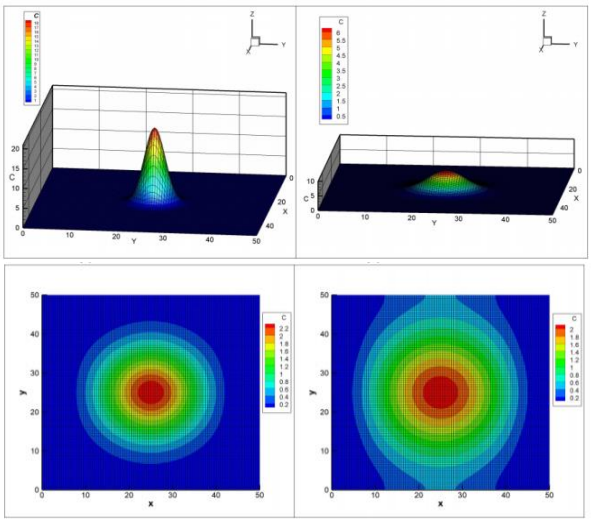

(c) The concentration of the tumor after five days (t = 50).

(d) The concentration of the tumor after five days (t = 100).

Figure 1. The depiction of glioma concentration in a 2-dimensional diffusion logistic model within a heterogeneous tissue environment is presented with respect to position at different time intervals.

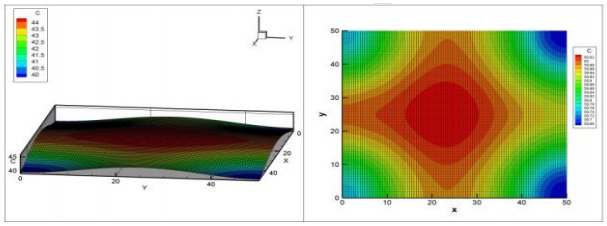

(c) The concentration of the tumor after five days (t = 650).

Figure 2. The diagram depicts the fluctuation of glioma tumor levels in a two-dimensional logistic diffusion model across a diverse tissue setting at various time points and positions.

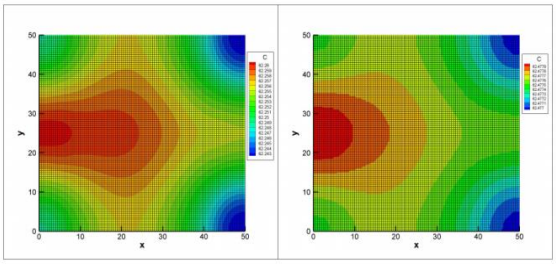

(a) The concentration of the tumor after five days (t = 1500) days.

(b) The concentration of the tumor after five days (t = 1700).days

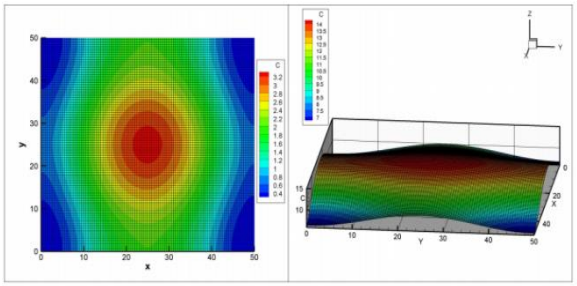

(c)The concentration of the tumor after five days (t = 15).

(d) The concentration of the tumor after five days (t = 450).

Figure 3. depicts the concentration of glioma tumor in a two-dimensional diffusion logistic model within a heterogeneous tissue environment, with respect to position at various time steps

7. CONCLUTION

Our study aims to introduce different variables into the model by considering spatial variation. This spatial variation is taken into account for the varying properties observed within the system. By integrating disparate tissue environments, we obtain a more comprehensive understanding of the behavior and dynamics of the model. These studies allow us to capture the complexity and detail of real-world scenarios, particularly regarding Gliomas of the brain. Overall, our results highlight the importance of considering spatial variability and its impact on the overall behavior of the system.

8. REFERENCES

1. D. G. Aronson and H. F. Weinberger, Nonlinear diffusion in population genetics, combustion, and nerve pulse propagation. In Partial differential equations and related topics, Springer, Berlin, Heidelberg, 1975, pp. 5-49.
2. D. G. Aronson and H. F. Weinberger, Multidimensional nonlinear diffusion arising in

population genetics. Advances in Mathematics, 30 (1978), 33-76.

3. W. Bao, Y. Du, Z. Lin and H. Zhu, Free boundary models for mosquito range movement driven by climate warming. Journal of Mathematical Biology, 76(2018), 841-875.
4. G. Bunting, Y. Du and K. Krakowski, Spreading speed revisited: analysis of a free boundary model. Networks and Heterogeneous Media, 7 (2012), 583-603.
5. K. Burrage and J. C. Butcher, Stability criteria for implicit Runge-Kutta methods.SIAM Journal on Numerical Analysis, 16 (1979), 46-57.
6. L. A. Caffarelli and S. Salsa, A Geometric Approach to Free Boundary Problems,American Mathematical Soc., 2005.
7. Y. Cao, A. Faghri and W. S. Chang, A numerical analysis of Stefan problems for generalized multi-dimensional phase-change structures using the enthalpytransforming model, International Journal of Heat and Mass Transfer, 32 (1989),1289-1298.
8. H. Chen, C. Min and F. Gibou, A numerical scheme for the Stefan problem on adaptive Cartesian grids with supralinear convergence rate, Journal of Computational Physics,228 (2009), 5803-5818.
9. S. Chen, B. Merriman, S. Osher and P. Smereka, A simple level set method for solving Stefan problems, Journal of Computational Physics, 135 (1997), 8-29.
10. S. Chen and Y. Zhang, Krylov implicit integration factor methods for spatial discretization on high dimensional unstructured meshes: application to discon-97tinuous Galerkin methods, Journal of Computational Physics, 230 (2011,(
11. I. L. Chern, J. Glimm, O. McBryan, B. Plohr and S. Yaniv, Front tracking forgas dynamics, Journal of Computational Physics, 62 (1986), 83-110.
12. J. Crank, Free and Moving Boundary Problems, Clarendon Press, Oxford, 1984.
13. Y. Du and Z. Guo, The Stefan problem for the Fisher-KPP equation, Journal of Differential Equations, 253 (2012), 996-1035.
14. Y. Du and Z. Lin, Spreading-vanishing dichotomy in the diffusive logistic model with a free boundary, SIAM Journal on Mathematical Analysis, 42 (2010), 377-405.
15. Y. Du and B. Lou, Spreading and vanishing in nonlinear diffusion problem with free boundaries, Journal of the European Mathematical Society, 17 (2015),2673-2724.
16. Y. Du, H. Matano and K.Wang, Regularity and asymptotic behavior of nonlinear Stefan problems, Archive for Rational Mechanics and Analysis, 212 (2014), 957-1010.
17. Y. Du and C.H. Wu, Spreading with two speeds and mass segregation in adiffusive competition system with free boundaries, Calculus of Variations and Partial Differential Equations, 57 (2018). https://doi.org/10.1007/s00526-018-
18. R. Fedkiw and S. Osher, Level Set Methods and Dynamic Implicit SurfacesApplied Mathematical Sciences, 153. Springer-Verlag, New York, 2003.
19. R. A. Fisher, The wave of advance of advantageous genes. Annals of eugenics, 7(1937), 355-369.
20. E. Gallopoulos and Y. Saad, Efficient solution of parabolic equations by Krylov approximation methods, SIAM Journal on Scientific and Statistical Computing,13 (1992), 1236–1264.
21. F. Gibou and R. Fedkiw, A fourth order accurate discretization for the Laplace and heat equations on arbitrary domains, with applications to the Stefan problem,Journal of Computational Physics, 202 (2005), 577-601.98
22. J. Glimm, X. L. Li, Y. Liu and N. Zhao, Conservative front tracking and level set algorithms, Proceedings of the National Academy of Sciences, 98 (2001), 14198-14201.
23. J.S. Guo and C.H. Wu, Dynamics for a two-species competition-diffusion modelwith two free boundaries, Nonlinearity 28 (2015), 1-27.
24. J.S. Guo and C.H. Wu, On a free boundary problem for a two-species weak competition system, Journal of Dynamics and Differential Equations, 24 (2012),873-895.
25. E. Hairer and G. Wanner, Stiff differential equations solved by Radau methods, Journal of Computational and Applied Mathematics, 111 (1999), 93-111.

Arabic Abstract

يقدم البحث تحليلاً عددياً مفصلاً لمعادلة التفاعل والانتشار غير الخطية ذات الرتبة الرابعة والكسورية باستخدام طريقة الفروق المضغوطة. إدخال المشتقة الكسورية من الرتبة الرابعة يضيف تعقيدًا إضافيًا للمعادلة، مما يجعل حلها التحليلي صعبًا. لذلك، يصبح النهج العددي ضروريًا لفهم سلوك المعادلة والحصول على حلول تقريبية. تُستخدم طريقة الفروق المضغوطة، المعروفة بدقتها وكفاءتها في حل المعادلات التفاضلية، لتقسيم المشتقات المكانية والزمنية للمعادلة. يتم تقريب المشتقات الكسورية باستخدام مشغلات فروق مناسبة. يتم حل النظام الناتج بشكل تكراري باستخدام تقنيات عددية مناسبة. تتناول الدراسة نموذجًا للتفاعل والانتشار يُستخدم في أورام الدماغ الجليومية، وتدمج وظيفتي انتشار مختلفتين. من أجل تحقيق فهم شامل، يتم توسيع التحليل ليشمل مختلف أنواع بيئات الأنسجة. يتم فحص سيناريوهات متنوعة، مع ثبات معامل الانتشار لتصوير بيئة أنسجة موحدة. علاوة على ذلك، يتم استكشاف الحالات التي يتغير فيها معامل الانتشار مكانيًا، مما يجلب التباين إلى النموذج. يتيح هذا التنوع المكاني استيعاب الخصائص المتباينة للمناطق المختلفة داخل الدماغ. بعد ذلك، يتم توسيع الدراسة لتشمل بيئات أنسجة متباينة في الأبعاد الثنائية..